The influences of El Niño–Southern Oscillation on tropospheric ozone in CMIP6 models

Thanh Le[1,2⋆], Seon-Ho Kim[2], Jae-Yeong Heo[2] and Deg-Hyo Bae[2⋆]

[1]Key Laboratory of Meteorological Disaster, Ministry of Education (KLME)/Collaborative Innovation Center on Forecast and Evaluation of Meteorological Disasters (CIC-FEMD), Nanjing University of Information Science and Technology, Nanjing 210044, China
[2]Department of Civil and Environmental Engineering, Sejong University, Seoul 05006, Republic of Korea

⋆Corresponding author(s): Thanh Le (levinhthanh.lvt@gmail.com) and Deg-Hyo Bae (dhbae@sejong.ac.kr)

Abstract. Ozone in the troposphere is a greenhouse gas and a pollutant, hence, additional understanding of the drivers of tropospheric ozone evolution is essential. The El Niño–Southern Oscillation (ENSO) is a main climate mode and may contribute to the variations of tropospheric ozone. Nevertheless, there is uncertainty regarding the causal influences of ENSO on tropospheric ozone under warming environment. Here, we investigated the links between ENSO and tropospheric ozone using Coupled Modeling Intercomparison Project Phase 6 (CMIP6) data over the period 1850-2014. Our results show that ENSO impacts on tropospheric ozone are primarily found over oceans, while the signature of ENSO over continents is largely nonsignificant. Springtime surface ozone is more sensitive to ENSO compared to other seasons. The response of ozone to ENSO may vary depending on specific air pressure levels in the troposphere. These responses are weak in the middle troposphere and are stronger in the upper and lower troposphere. ~~Although there are biases~~There is high consistency across CMIP6 models in simulating the signature of ENSO on ~~surface~~ ozone over ~~, these signatures in~~ the lower, middle and upper troposphere ~~appear to be more consistent across CMIP6 models~~. While the response of tropical tropospheric ozone to ENSO is in agreement with previous works, our results suggest that ENSO impacts on tropospheric ozone over the northern North Pacific, American continent, and over~~of~~ the mid-latitude regions of~~over~~ the southern Pacific, Atlantic, and Indian oceans might be more significant than previously understood.

Keywords: El Niño–Southern Oscillation; historical simulations; tropospheric ozone; interactive chemistry; CMIP6.

1 Introduction

Ozone in the troposphere is an important greenhouse gas and pollutant (Archibald et al., 2020; Cooper et al., 2010; Wang et al., 2022). Tropospheric ozone has detrimental effects on human health and ecosystems (Fleming et al., 2018; Franz et al., 2018; Gaudel et al., 2020; Lu et al., 2019; Oliver et al., 2018; Peron et al., 2021; Roberts et al., 2022; Schauberger et al., 2019). Changes in atmospheric ozone may also affect radiative forcing and have effects on climate (Gauss et al., 2006; Myhre et al., 2013).

The El Niño–Southern Oscillation (ENSO) is the major mode of climate variability with global impacts (Bjerknes, 1969; Cai et al., 2020; McPhaden et al., 2006) and is expected to affect variations of global tropospheric ozone. ENSO-induced changes in climate and meteorological conditions (Le and Bae, 2022a; Lu et al., 2019; Yeh et al., 2018) lead to impacts on ecosystems and the production/removal of ozone in soil, plant, and the water cycle, and the transport of ozone (Ganzeveld et al., 2009; Lin et al., 2019; Neu et al., 2014). In particular, ENSO drives changes in tropospheric and stratospheric circulations which can alter the tropospheric ozone variations (Daskalakis et al., 2022; Domeisen et al., 2019; Koumoutsaris et al., 2008; Lin et al., 2015; Neu et al., 2014; Olsen et al., 2019; Oman et al., 2013; Zeng and Pyle, 2005; Ziemke et al., 2015). In addition, ENSO was revealed to exhibit influences on tropospheric ozone concentrations in many regions by modulating local meteorological conditions (Doherty et al., 2006; Jeong et al., 2023; Jiang and Li, 2022; Oman et al., 2011; Peiro et al., 2018; Rowlinson et al., 2019; Wie et al., 2021; Xu et al., 2017; Yang et al., 2022; Zhang et al., 2015).

Nevertheless, there are uncertainties regarding the causal effects of ENSO on global tropospheric ozone. For instance, while the response of tropospheric ozone to ENSO over the mid-latitude regions remains elusive (Lu et al., 2019; Olsen et al., 2016), further understanding of ENSO impacts on ozone concentrations at multiple air pressure levels in the troposphere is necessary. Moreover, a causal analysis (Le et al., 2022; Le and Bae, 2022b) that takes into account the confounding impacts of other climate modes on the relationship between ENSO and tropospheric ozone is lacking. While the response of tropospheric ozone to ENSO can be interpreted by changes in ENSO-related atmospheric circulation (Lu et al., 2019; Sekiya and Sudo, 2012; Ziemke and Chandra, 2003), these changes might be influenced by other climate modes (Cai et al., 2019; Le et al., 2020b). Despite the high spatial and temporal variability of tropospheric ozone, there are limited observations of past ozone changes at the global scale (Dragani, 2011; Ebojie et al., 2016; Gaudel et al., 2018; Young et al., 2018). Hence, Earth system models remain valuable tools to understand the evolution of tropospheric ozone and the interactions between tropospheric ozone and regional climate (Archibald et al., 2020; Collins et al., 2017; Young et al., 2018). Datasets from Coupled Modeling Intercomparison Project Phase 6 (CMIP6) models provide an important source to better identify the effects of ENSO on global tropospheric ozone.

In the present study, we evaluated the causal impacts of ENSO on tropospheric ozone at the global scale using data from the historical simulations of CMIP6 models. We also discussed the coherency across CMIP6 models in reproducing the connection between ENSO and tropospheric ozone.

2 Materials and Methods

2.1 Datasets

We used monthly data of mole fraction of ozone in air (i.e., variable ‘o3’) at different air pressure levels (i.e., 1000, 850, 500, and 300 hPa). The CMIP6 models with ozone data available for the historical simulations (Eyring et al., 2016) over the 1850-2014 period are listed in Table 1. In Table 1, the models equipped with an Atmospheric Chemistry module are fully coupled where the chemistry scheme is associated with the physics of the atmospheric model, allowing for comprehensive

consideration of interactions between climate variations, interactive chemistry, and carbon cycle (Emmons et al., 2020; Michou et al., 2020; Wu et al., 2019). The use of various model outputs reduces the uncertainty of the connections between ENSO and tropospheric ozone.

There are biases in simulating tropospheric ozone variations in the models (Griffiths et al., 2021; Turnock et al., 2020; Young et al., 2018). For instance, CMIP6 models may underestimate ozone levels in the Southern Hemisphere and overestimate ozone levels in the Northern Hemisphere compared to observational data of recent past (Griffiths et al., 2021; Turnock et al., 2020; Young et al., 2018). However, CMIP model outputs are still helpful to investigate the effects of ENSO on tropospheric ozone (Archibald et al., 2020; Young et al., 2018). For example, the simulation of tropospheric ozone in CESM2 models is improved in comparison to previous model versions (Emmons et al., 2020). In addition, CMIP6 models are capable of simulating long-term changes in surface ozone levels and recent increasing trends in tropospheric ozone (Griffiths et al., 2021; Turnock et al., 2020).

We employed monthly sea level pressure (SLP) and sea surface temperature (SST) to calculate the time series of the major climate modes (see also section Methods 2.2).

Table 1. List of CMIP6 models used in this study.

No.	Model name	Modelling center, country	Atmospheric Chemistry model
1	BCC_CSM2_MR	BCC, China	None
2	BCC_ESM1	BCC, China	BCC-AGCM3-Chem
3	CESM2	NCAR, United States	MOZART-T1
4	CESM2_FV2	NCAR, United States	MOZART-T1
5	CESM2_WACCM	NCAR, United States	MOZART-T1
6	CESM2_WACCM_FV2	NCAR, United States	MOZART-T1
7	CNRM_CM6_1	CNRM-CERFACS, France	OZL_v2
8	CNRM_CM6_1_HR	CNRM-CERFACS, France	OZL_v2
9	CNRM_ESM2_1	CNRM-CERFACS, France	REPROBUS-C_v2
10	IPSL_CM6A_LR	IPSL, France	None
11	MPI_ESM_1_2_HAM	MPI-M, Germany	Sulfur chemistry (unnamed)
12	MPI_ESM1_2_LR	MPI-M, Germany	None

2.2 Methods

We assess the possibility of the impacts of ENSO on tropospheric ozone based on the approach employed in recent studies (Le and Bae, 2020, 2022a). This method was established using a multivariate predictive model to assess the probability for the absence of Granger causal effects of ENSO on ozone concentrations. In the computations, we considered the confounding impacts of other major climate modes (i.e., the dipole mode index (DMI; Saji et al., 1999), the Southern Annular Mode (SAM; e.g., Cai et al., 2011), and the North Atlantic Oscillation (NAO; e.g., Hurrell et al., 2003)). Given that the climate changes in the Indian and Atlantic oceans can affect the tropical Pacific (Cai et al., 2019; Ha et al., 2017a; Le et al., 2020a; Le and Bae, 2019), and modify the connections between ENSO and ozone concentrations, these analyses provide a realistic estimate for the response of ozone concentrations to ENSO.

We use the following multivariate predictive model (e.g., Stern and Kaufmann 2013, Mosedale *et al* 2006) to estimate the causal links between the ENSO and ozone concentration:

$$\boldsymbol{X_t = \sum_{i=1}^{p} \alpha_i X_{t-i} + \sum_{i=1}^{p} \beta_i Y_{t-i} + \sum_{j=1}^{m} \sum_{i=1}^{p} \delta_{j,i} Z_{j,t-i} + \varepsilon_t} \quad \textbf{(1)}$$

where X_t is the annual mean (or seasonal mean) ozone concentration for year t, Y_t is the ENSO index, and $Z_{j,t}$ is the confounding factor j for year t. In the predictive model shown in equation 1, while estimating the influence of Y on X (i.e., the contribution of the term $\sum_{i=1}^{p} \beta_i Y_{t-i}$ in predicting X), the contribution of past X events are already taken into account by adding the term $\sum_{i=1}^{p} \alpha_i X_{t-i}$. Thus, the causal influence of Y on X, if detected, is robust and the contribution of past X events are already considered in our analyses. Here, m is number of confounding factors and $p \geq 1$ is the order of the multivariate predictive model. The optimal order p is computed by minimizing the Schwarz criterion or the Bayesian information criterion (Schwarz, 1978). The optimal orders might be different for each model.

The ENSO index was computed as the average sea surface temperature (SST) anomalies in the Niño 3.4 area (120–170°W; 5°N–5°S) in boreal winter (December–January–February, DJF). Confounding factors (i.e., the dipole mode index (DMI; Saji et al., 1999), the Southern Annular Mode (SAM) and the North Atlantic Oscillation (NAO; e.g., Hurrell et al., 2003)) may have effects on the connections between ENSO and ozone concentration. The DMI was given as the difference in boreal fall (September–October–November, SON) SST anomalies between two Indian Ocean regions of the western pole (50–70°E; 10°N–10°S) and southeastern pole (90–110°E; 0°N–10°S). The SAM (Cai et al., 2011) was calculated as the first empirical orthogonal function (EOF) of the boreal summer (June–July–August, JJA) sea level pressure (SLP) anomalies for the region of 40–70°S. The NAO index is computed as the EOF of boreal winter (DJF) SLP anomalies in the North Atlantic area (90ºW-40ºE, 20º-70ºN). In this study, the confounding factors are limited to three major climate modes (i.e., DMI, SAM and NAO) as these modes are crucial to global climate variability on interannual time scales (Delworth et al., 2016; Hurrell et al., 2003; Kripalani et al., 2009; Luo et al., 2012; Raphael and Holland, 2006). Furthermore, alterations in these climate modes may influence the variations of ENSO (Cai et al., 2019; Ha et al., 2017b; Le et al., 2020b; Le and Bae, 2019).

We estimate the probability of no Granger causality by applying a test of Granger causality (Le and Bae, 2020; Mosedale et al., 2006; Stern and Kaufmann, 2013) for the multivariate predictive model shown in equation 1. For computing the degree of uncertainty, we followed recent guidance (Stocker et al., 2013) and utilized the terms 'very unlikely', 'unlikely', 'likely' for the 0–10%, 0–33%, and 66–100% probability of the likelihood of the outcome, respectively. For example, if the *p*-value is less than 0.33, the result indicates that ENSO is unlikely to display no Granger causality on ozone concentration. In this instance, we conclude that ENSO has 'causal effect' on ozone concentration.

3 Results

Figure 1 depicts the models' mean map of ozone concentrations at different air pressure levels for the period 1850-2014 of the CMIP6 historical simulations. As we will show in Figure 3, the models without the Atmospheric Chemistry module (i.e., 4 models numbered 1, 10, 11 and 12 in Table 1) exhibit distinct outcomes of ENSO impacts compared to both the models' mean and the remaining models. Hence, it's important to note that the models' mean is solely derived from the results obtained from all the models equipped with an Atmospheric Chemistry module (i.e., 8 models numbered from 2 to 9 in Table 1). In the middle and lower troposphere, ozone is higher in the northern hemisphere compared to the southern hemisphere (Figure 1). The agreement between models fluctuates at different air pressure levels. For example, in the upper troposphere (i.e., at 300 hPa pressure level), high consistency across the model is found in the mid-latitude regions, while this consistency is lower in the tropics and polar regions (Figure 1a). In the middle troposphere (i.e., at 500 hPa pressure level), the models' agreement is mainly found in the northern hemisphere (Figure 1b). The simulations of near-surface ozone (i.e., at 850 hPa) are consistent over ~~the tropics and~~ parts of the northern hemisphere (Figure 1c), while the models' agreement is low in reproducing surface ozone (i.e., at 1000 hPa) for most regions (Figure 1d). The standard deviation is normally higher in the tropics and much of the southern hemisphere compared to other regions (Figure S1).

Figure 2 displays the causal effects of ENSO on global ozone concentrations for the historical period 1850-2014. In Figure 2, we show that the response of ozone to ENSO may vary depending on specific air pressure level. For instance, ENSO impacts on ozone in the upper troposphere (i.e., at 300 hPa pressure level) can be observed over the tropics, parts of the Pacific Ocean, South America and North America (Figure 2a). In these areas, ENSO is unlikely to exhibit no causal influences on ozone concentrations (i.e., *p*-values were lower than 0.33). Further analysis (not shown) indicates that the patterns of ENSO impacts on ozone at 250 hPa are similar to those at 300 hPa. This implies that the response of ozone variation to ENSO might remain consistent across the upper troposphere, the tropopause, and the lower stratosphere. The response of ozone to ENSO in the middle troposphere (i.e., at 500 hPa pressure level) is ~~very limited~~found over the tropical Pacific and Atlantic Oceans (Figure 2b). We observe more significant impacts of ENSO on ozone in the lower troposphere compared to the upper and middle troposphere. Specifically, tropical ozone concentrations at near surface (i.e., at 850 hPa) and surface (i.e., at 1000 hPa) levels appear to be sensitive to ENSO (Figures 2c and d). In these regions, ENSO is very unlikely to exhibit no causal influences on ozone concentrations (i.e., *p*-values were lower than 0.1). In addition, ENSO impacts on surface ozone can be

found over part of the northern North Pacific and mid-latitude regions in the southern hemisphere (Figure 2d). ~~We observe causal influences of ENSO on ozone over Antarctica, however, these influences show low agreement between models (Figures 2c and d).~~ While the signature of ENSO on ozone variations is generally weak over continents of the lower and middle troposphere (Figures 2b-d), this signature is, however, stronger in the upper troposphere over North America (Figure 2a). These results imply that the effects of ENSO on tropospheric ozone over lands are nonsignificant for most regions.

Differences between CMIP6 models in replicating the influences of ENSO on surface (1000 hPa) ozone are shown in Figure 3. Similar results for other pressure levels (300, 500, and 850 hPa) are presented in Figures S2-S4. As revealed in Figure 3, several models (i.e., BCC_CSM2_MR, IPSL_CM6A_LR, and MPI_ESM1_2_LR) may not reproduce the significant influences of ENSO on surface ozone over the tropical Pacific and Indian Oceans as described in Figure 2d. The models IPSL_CM6A_LR and MPI_ESM1_2_LR may underestimate the response of surface ozone to ENSO over the mid-latitude regions in the southern hemisphere compared to other models. The agreement between models for the impacts of ENSO on surface ozone is low over continents (Figure 2d), partly due to the discrepancy in simulating ozone variability (Figure 1d). While there are biases in simulating the response of surface ozone to ENSO (Figure 2d), these responses in the middle and upper troposphere appear to be more consistent across models (Figures 2a-c, S2-4).

Springtime surface ozone is more sensitive to ENSO compared to other seasons (Figure 4). In particular, the clear response of springtime surface ozone over the tropics, the high-latitude north Pacific and the mid to high-latitude of the southern hemisphere can be observed (Figure 4a). The impacts of ENSO on surface ozone of other seasons are limited (e.g., over the tropical Pacific and part of southern North America, Figure 4b-d). The results for other air pressure levels (300, 500, and 850 hPa) are shown in Figures S5-S7. We note that the response of springtime ozone at higher pressure levels is weaker compared to springtime surface ozone for most regions, except for the upper troposphere over east Asia, northern South America and northwestern North America (Figure S5a). Consistent with the results illustrated in Figure 2b, the impacts of ENSO on seasonal ozone in the middle troposphere (500 hPa) are ~~largely~~ mainly ~~non~~significant ~~for all seasons~~over the tropics and part of northern North Pacific (Figure S6).

4 Discussion and conclusions

The effects of ENSO on tropospheric ozone over the tropical Pacific (Figures 2-4) show agreement with previous works (Chandra et al., 2007; Peiro et al., 2018). ENSO causes changes in the tropospheric ozone budget over the tropical Pacific by modulating the Walker circulation (Chandra et al., 2007), wind systems (Cai et al., 2021; Le and Bae, 2020; Yeh et al., 2018), and inducing biomass burning (Chandra et al., 2009; Le et al., 2022). Further, significant ENSO impacts on tropical ocean regions described in Figures 2-4 are in agreement with recent works (Olsen et al., 2016; Wespes et al., 2017) using satellite data.

Despite the limited consensus among models in replicating ozone levels in the lower troposphere, and a high standard deviation particularly in tropical regions, (Figures 1 and S1), we observed noteworthy effects of ENSO on lower

tropospheric ozone (Figure 2). These results exhibit a degree of independence and are not contradictory. This is because the models' mean of annual ozone is calculated over the entire 1850-2014 period, whereas the assessment of the relationship between the ENSO and annual ozone is conducted on a year-to-year basis. Furthermore, variations in ozone are also influenced by factors beyond ENSO, including other major climate modes, cyclones, and local emissions of ozone precursors such as nitrogen oxides (NO_x), volatile organic compounds, and carbon monoxide (CO). Biases in simulating these factors contribute to the inconsistencies of ozone in the models, although there is consensus in simulating the connection between ENSO and ozone.

The significant impacts of ENSO on ozone in the upper troposphere (300 hPa) over the southern and western North America (Figures 2a and S5a) might be associated with the transport of ozone from east Asia (Cooper et al., 2010; Doherty, 2015; Lin et al., 2015). These impacts can be explained by the modulation of ENSO on springtime upper tropospheric ozone over east Asia (Figure S5a) and the connection between ENSO and the North Pacific Oscillation (Kug et al., 2020). However, these impacts cannot reach the surface levels (Figures 2c-d, ~~S6a,~~ and S7a), consistent with recent work (Lin et al., 2015).

We note that the models without the Atmospheric Chemistry module (BCC_CSM2_MR, IPSL_CM6A_LR, MPI_ESM_1_2_HAM, and MPI_ESM1_2_LR; See Table 1) provide different results of ENSO impacts compared to the rest models (Figures 3). In these models, ozone variations are prescribed using observational data (Lurton et al., 2020; Wu et al., 2019), and it is expected that the response of ozone variation to atmospheric circulation and ENSO is not significant. Hence, improvement of the Atmospheric Chemistry module in the models may provide further understanding of the connection between ENSO and ozone variations.

The robust response of lower tropospheric ozone to ENSO is associated with ENSO-induced changes in the atmospheric circulation (Oman et al., 2011) and this response is particularly prominent over the tropics (Figures 2c and d). However, this response appears to be weaker over the middle and upper troposphere (Figures 2a and b). The weak impacts of ENSO on the mid-level tropospheric ozone (i.e., 500 hPa level, described in Figures 2b) might be due to the strong exchange between stratospheric ozone and middle to upper tropospheric ozone (Liu et al., 2017; Meul et al., 2018; Neu et al., 2014; Williams et al., 2019). The more pronounced reaction of upper tropospheric ozone to ENSO in comparison to middle tropospheric ozone could be attributed to the influence of ENSO on deep convective transport and the interconnected relationship between ENSO and the North Pacific Oscillation (Cai et al., 2019; Gaudel et al., 2020; Kug et al., 2020).

Several models showed ENSO effects on tropospheric ozone over Antarctica with a low agreement between models (Figures 2-4). These impacts might be associated with the signature of ENSO on stratospheric ozone anomalies over Antarctica (Li et al., 2021; Lin and Qian, 2019).

Given that the tropospheric ozone burden and the ozone-induced impacts may increase in some regions in the future (Doherty et al., 2013; Franz and Zaehle, 2021; Gaudel et al., 2020; Griffiths et al., 2021; Verstraeten et al., 2015; Zanis et al., 2022), further analyses of ENSO impacts on tropospheric ozone in future climate projections are necessary. In addition, as the tropopause may vary depending on different latitudes (Griffiths et al., 2021), it is essential to conduct further analyses

that specifically address the impacts of ENSO on ozone concentrations across the upper troposphere, the tropopause, and the lower stratosphere.

Acknowledgments

The authors thank editor Graciela Raga and the anonymous reviewers for their valuable comments and suggestions. We acknowledge the World Climate Research Programme, which through its Working Group on Coupled Modelling, coordinated and promoted CMIP6. We thank the climate modelling groups (listed in Table 1) for producing and making available their model output, the Earth System Grid Federation (ESGF) for archiving the data and providing access, and the multiple funding agencies who support CMIP6 and ESGF. Thanh Le is supported by the Startup Foundation for Introducing Talent of Nanjing University of Information Science and Technology (NUIST) and by the National Research Foundation of Korea (NRF) grant funded by the Korea government (MSIT) (Grant No. 2021R1G1A1004389).

Data Availability

The data that support the findings of this study are openly available at the following website: https://esgf-node.llnl.gov/search/cmip6/.

Author contribution

TL designed the study, performed the data analysis, and wrote the manuscript. SHK, JYH and DHB contributed to the interpretation of results and the writing of the manuscript.

Competing interests

The authors declare that they have no conflict of interest.

Financial support

This work is by the Startup Foundation for Introducing Talent of Nanjing University of Information Science and Technology (NUIST) and supported by the National Research Foundation of Korea (NRF) grant funded by the Korea government (MSIT) (Grant No. 2021R1G1A1004389).

References

Archibald, A. T., Neu, J. L., Elshorbany, Y. F., Cooper, O. R., Young, P. J., Akiyoshi, H., Cox, R. A., Coyle, M., Derwent, R. G., Deushi, M., Finco, A., Frost, G. J., Galbally, I. E., Gerosa, G., Granier, C., Griffiths, P. T., Hossaini, R., Hu, L., Jöckel, P., Josse, B., Lin, M. Y., Mertens, M., Morgenstern, O., Naja, M., Naik, V., Oltmans, S., Plummer, D. A., Revell, L. E., Saiz-Lopez, A., Saxena, P., Shin, Y. M., Shahid, I., Shallcross, D., Tilmes, S., Trickl, T., Wallington, T. J., Wang, T., Worden, H. M. and Zeng, G.: Tropospheric Ozone Assessment Report, Elem. Sci. Anthr., 8(1), 1–53, doi:10.1525/elementa.2020.034, 2020.

Bjerknes, J.: Atmospheric teleconnections from the equatorial Pacific, Mon. Weather Rev., 97(3), 163–172, doi:10.1175/1520-0493(1969)097<0163:ATFTEP>2.3.CO;2, 1969.

Cai, W., Sullivan, A. and Cowan, T.: Interactions of ENSO, the IOD, and the SAM in CMIP3 Models, J. Clim., 24(6), 1688–1704, doi:10.1175/2010JCLI3744.1, 2011.

Cai, W., Wu, L., Lengaigne, M., Li, T., McGregor, S., Kug, J.-S., Yu, J.-Y., Stuecker, M. F., Santoso, A., Li, X., Ham, Y.-G., Chikamoto, Y., Ng, B., McPhaden, M. J., Du, Y., Dommenget, D., Jia, F., Kajtar, J. B., Keenlyside, N., Lin, X., Luo, J.-J., Martín-Rey, M., Ruprich-Robert, Y., Wang, G., Xie, S.-P., Yang, Y., Kang, S. M., Choi, J.-Y., Gan, B., Kim, G.-I., Kim, C.-E., Kim, S., Kim, J.-H. and Chang, P.: Pantropical climate interactions, Science (80-.)., 363(6430), eaav4236, doi:10.1126/science.aav4236, 2019.

Cai, W., McPhaden, M. J., Grimm, A. M., Rodrigues, R. R., Taschetto, A. S., Garreaud, R. D., Dewitte, B., Poveda, G., Ham, Y.-G., Santoso, A., Ng, B., Anderson, W., Wang, G., Geng, T., Jo, H.-S., Marengo, J. A., Alves, L. M., Osman, M., Li, S., Wu, L., Karamperidou, C., Takahashi, K. and Vera, C.: Climate impacts of the El Niño–Southern Oscillation on South America, Nat. Rev. Earth Environ., 1(4), 215–231, doi:10.1038/s43017-020-0040-3, 2020.

Cai, W., Santoso, A., Collins, M., Dewitte, B., Karamperidou, C., Kug, J.-S., Lengaigne, M., McPhaden, M. J., Stuecker, M. F., Taschetto, A. S., Timmermann, A., Wu, L., Yeh, S.-W., Wang, G., Ng, B., Jia, F., Yang, Y., Ying, J., Zheng, X.-T., Bayr, T., Brown, J. R., Capotondi, A., Cobb, K. M., Gan, B., Geng, T., Ham, Y.-G., Jin, F.-F., Jo, H.-S., Li, X., Lin, X., McGregor, S., Park, J.-H., Stein, K., Yang, K., Zhang, L. and Zhong, W.: Changing El Niño–Southern Oscillation in a warming climate, Nat. Rev. Earth Environ., 2(9), 628–644, doi:10.1038/s43017-021-00199-z, 2021.

Chandra, S., Ziemke, J. R., Schoeberl, M. R., Froidevaux, L., Read, W. G., Levelt, P. F. and Bhartia, P. K.: Effects of the 2004 El Niño on tropospheric ozone and water vapor, Geophys. Res. Lett., 34(6), L06802, doi:10.1029/2006GL028779, 2007.

Chandra, S., Ziemke, J. R., Duncan, B. N., Diehl, T. L., Livesey, N. J. and Froidevaux, L.: Effects of the 2006 El Niño on tropospheric ozone and carbon monoxide: implications for dynamics and biomass burning, Atmos. Chem. Phys., 9(13), 4239–4249, doi:10.5194/acp-9-4239-2009, 2009.

Collins, W. J., Lamarque, J.-F., Schulz, M., Boucher, O., Eyring, V., Hegglin, M. I., Maycock, A., Myhre, G., Prather, M., Shindell, D. and Smith, S. J.: AerChemMIP: quantifying the effects of chemistry and aerosols in CMIP6, Geosci. Model Dev., 10(2), 585–607, doi:10.5194/gmd-10-585-2017, 2017.

Cooper, O. R., Parrish, D. D., Stohl, A., Trainer, M., Nédélec, P., Thouret, V., Cammas, J. P., Oltmans, S. J., Johnson, B. J., Tarasick, D., Leblanc, T., McDermid, I. S., Jaffe, D., Gao, R., Stith, J., Ryerson, T., Aikin, K., Campos, T., Weinheimer, A. and Avery, M. A.: Increasing springtime ozone mixing ratios in the free troposphere over western North America, Nature, 463(7279), 344–348, doi:10.1038/nature08708, 2010.

Daskalakis, N., Gallardo, L., Kanakidou, M., Nüß, J. R., Menares, C., Rondanelli, R., Thompson, A. M. and Vrekoussis, M.: Impact of biomass burning and stratospheric intrusions in the remote South Pacific Ocean troposphere, Atmos. Chem. Phys., 22(6), 4075–4099, doi:10.5194/acp-22-4075-2022, 2022.

Delworth, T. L., Zeng, F., Vecchi, G. A., Yang, X., Zhang, L. and Zhang, R.: The North Atlantic Oscillation as a driver of rapid climate change in the Northern Hemisphere, Nat. Geosci., 9(June), 509–512, doi:10.1038/ngeo2738, 2016.

Doherty, R. M.: Ozone pollution from near and far, Nat. Geosci., 8(9), 664–665, doi:10.1038/ngeo2497, 2015.

Doherty, R. M., Stevenson, D. S., Johnson, C. E., Collins, W. J. and Sanderson, M. G.: Tropospheric ozone and El Niño–Southern Oscillation: Influence of atmospheric dynamics, biomass burning emissions, and future climate change, J. Geophys. Res., 111(D19), D19304, doi:10.1029/2005JD006849, 2006.

Doherty, R. M., Wild, O., Shindell, D. T., Zeng, G., MacKenzie, I. A., Collins, W. J., Fiore, A. M., Stevenson, D. S., Dentener, F. J., Schultz, M. G., Hess, P., Derwent, R. G. and Keating, T. J.: Impacts of climate change on surface ozone and intercontinental ozone pollution: A multi-model study, J. Geophys. Res. Atmos., 118(9), 3744–3763, doi:10.1002/jgrd.50266, 2013.

Domeisen, D. I. V., Garfinkel, C. I. and Butler, A. H.: The Teleconnection of El Niño Southern Oscillation to the Stratosphere, Rev. Geophys., 57(1), 5–47, doi:10.1029/2018RG000596, 2019.

Dragani, R.: On the quality of the ERA-Interim ozone reanalyses: comparisons with satellite data, Q. J. R. Meteorol. Soc., 137(658), 1312–1326, doi:10.1002/qj.821, 2011.

Ebojie, F., Burrows, J. P., Gebhardt, C., Ladstätter-Weißenmayer, A., von Savigny, C., Rozanov, A., Weber, M. and Bovensmann, H.: Global tropospheric ozone variations from 2003 to 2011 as seen by SCIAMACHY, Atmos. Chem. Phys., 16(2), 417–436, doi:10.5194/acp-16-417-2016, 2016.

Emmons, L. K., Schwantes, R. H., Orlando, J. J., Tyndall, G., Kinnison, D., Lamarque, J. F., Marsh, D., Mills, M. J., Tilmes, S., Bardeen, C., Buchholz, R. R., Conley, A., Gettelman, A., Garcia, R., Simpson, I., Blake, D. R., Meinardi, S. and Pétron, G.: The Chemistry Mechanism in the Community Earth System Model Version 2 (CESM2), J. Adv. Model. Earth Syst., 12(4), 1–21, doi:10.1029/2019MS001882, 2020.

Eyring, V., Bony, S., Meehl, G. A., Senior, C. A., Stevens, B., Stouffer, R. J. and Taylor, K. E.: Overview of the Coupled Model Intercomparison Project Phase 6 (CMIP6) experimental design and organization, Geosci. Model Dev., 9(5), 1937–1958, doi:10.5194/gmd-9-1937-2016, 2016.

Fleming, Z. L., Doherty, R. M., Von Schneidemesser, E., Malley, C. S., Cooper, O. R., Pinto, J. P., Colette, A., Xu, X., Simpson, D., Schultz, M. G., Lefohn, A. S., Hamad, S., Moolla, R., Solberg, S. and Feng, Z.: Tropospheric Ozone Assessment Report: Present-day ozone distribution and trends relevant to human health, Elementa, 6, doi:10.1525/elementa.273, 2018.

Franz, M. and Zaehle, S.: Competing effects of nitrogen deposition and ozone exposure on northern hemispheric terrestrial carbon uptake and storage, 1850-2099, Biogeosciences, 18(10), 3219–3241, doi:10.5194/bg-18-3219-2021, 2021.

Franz, M., Alonso, R., Arneth, A., Büker, P., Elvira, S., Gerosa, G., Emberson, L., Feng, Z., Le Thiec, D., Marzuoli, R., Oksanen, E., Uddling, J., Wilkinson, M. and Zaehle, S.: Evaluation of simulated ozone effects in forest ecosystems against biomass damage estimates from fumigation experiments, Biogeosciences, 15(22), 6941–6957, doi:10.5194/bg-15-6941-2018, 2018.

Ganzeveld, L., Helmig, D., Fairall, C. W., Hare, J. and Pozzer, A.: Atmosphere-ocean ozone exchange: A global modeling study of biogeochemical, atmospheric, and waterside turbulence dependencies, Global Biogeochem. Cycles, 23(4), n/a-n/a, doi:10.1029/2008GB003301, 2009.

Gaudel, A., Cooper, O. R., Ancellet, G., Barret, B., Boynard, A., Burrows, J. P., Clerbaux, C., Coheur, P.-F., Cuesta, J., Cuevas, E., Doniki, S., Dufour, G., Ebojie, F., Foret, G., Garcia, O., Granados-Muñoz, M. J., Hannigan, J. W., Hase, F., Hassler, B., Huang, G., Hurtmans, D., Jaffe, D., Jones, N., Kalabokas, P., Kerridge, B., Kulawik, S., Latter, B., Leblanc, T., Le Flochmoën, E., Lin, W., Liu, J., Liu, X., Mahieu, E., McClure-Begley, A., Neu, J. L., Osman, M., Palm, M., Petetin, H., Petropavlovskikh, I., Querel, R., Rahpoe, N., Rozanov, A., Schultz, M. G., Schwab, J., Siddans, R., Smale, D., Steinbacher, M., Tanimoto, H., Tarasick, D. W., Thouret, V., Thompson, A. M., Trickl, T., Weatherhead, E., Wespes, C., Worden, H. M., Vigouroux, C., Xu, X., Zeng, G. and Ziemke, J.: Tropospheric Ozone Assessment Report: Present-day distribution and trends of tropospheric ozone relevant to climate and global atmospheric chemistry model evaluation, edited by D. Helmig

and A. Lewis, Elem. Sci. Anthr., 6, doi:10.1525/elementa.291, 2018.

Gaudel, A., Cooper, O. R., Chang, K.-L., Bourgeois, I., Ziemke, J. R., Strode, S. A., Oman, L. D., Sellitto, P., Nédélec, P., Blot, R., Thouret, V. and Granier, C.: Aircraft observations since the 1990s reveal increases of tropospheric ozone at multiple locations across the Northern Hemisphere, Sci. Adv., 6(34), 1–12, doi:10.1126/sciadv.aba8272, 2020.

Gauss, M., Myhre, G., Isaksen, I. S. A., Grewe, V., Pitari, G., Wild, O., Collins, W. J., Dentener, F. J., Ellingsen, K., Gohar, L. K., Hauglustaine, D. A., Iachetti, D., Lamarque, F., Mancini, E., Mickley, L. J., Prather, M. J., Pyle, J. A., Sanderson, M. G., Shine, K. P., Stevenson, D. S., Sudo, K., Szopa, S. and Zeng, G.: Radiative forcing since preindustrial times due to ozone change in the troposphere and the lower stratosphere, Atmos. Chem. Phys., 6(3), 575–599, doi:10.5194/acp-6-575-2006, 2006.

Griffiths, P. T., Murray, L. T., Zeng, G., Shin, Y. M., Abraham, N. L., Archibald, A. T., Deushi, M., Emmons, L. K., Galbally, I. E., Hassler, B., Horowitz, L. W., Keeble, J., Liu, J., Moeini, O., Naik, V., O'Connor, F. M., Oshima, N., Tarasick, D., Tilmes, S., Turnock, S. T., Wild, O., Young, P. J. and Zanis, P.: Tropospheric ozone in CMIP6 simulations, Atmos. Chem. Phys., 21(5), 4187–4218, doi:10.5194/acp-21-4187-2021, 2021.

Ha, K.-J., Chu, J.-E., Lee, J.-Y. and Yun, K.-S.: Interbasin coupling between the tropical Indian and Pacific Ocean on interannual timescale: observation and CMIP5 reproduction, Clim. Dyn., 48(1–2), 459–475, doi:10.1007/s00382-016-3087-6, 2017a.

Ha, K.-J., Chu, J.-E., Lee, J.-Y. and Yun, K.-S.: Interbasin coupling between the tropical Indian and Pacific Ocean on interannual timescale: observation and CMIP5 reproduction, Clim. Dyn., 48(1–2), 459–475, doi:10.1007/s00382-016-3087-6, 2017b.

Hurrell, J. W., Kushnir, Y., Ottersen, G. and Visbeck, M.: An overview of the North Atlantic Oscillation, in Geophysical Monograph American Geophysical Union, pp. 1–35, American Geophysical Union., 2003.

Jeong, Y., Kim, S., Kim, J., Shin, D., Kim, J., Park, J. and An, S.: Influence of ENSO on Tropospheric Ozone Variability in East Asia, J. Geophys. Res. Atmos., 128(16), 1–18, doi:10.1029/2023JD038604, 2023.

Jiang, Z. and Li, J.: Impact of eastern and central Pacific El Niño on lower tropospheric ozone in China, Atmos. Chem. Phys., 22(11), 7273–7285, doi:10.5194/acp-22-7273-2022, 2022.

Koumoutsaris, S., Bey, I., Generoso, S. and Thouret, V.: Influence of El Niño–Southern Oscillation on the interannual variability of tropospheric ozone in the northern midlatitudes, J. Geophys. Res., 113(D19), D19301, doi:10.1029/2007JD009753, 2008.

Kripalani, R. H., Oh, J. H. and Chaudhari, H. S.: Delayed influence of the Indian Ocean Dipole mode on the East Asia-West Pacific monsoon: possible mechanism, Int. J. Climatol., 30(2), 197–209, doi:10.1002/joc.1890, 2009.

Kug, J., Vialard, J., Ham, Y., Yu, J. and Lengaigne, M.: ENSO Remote Forcing, pp. 247–265., 2020.

Le, T. and Bae, D.-H.: Response of global evaporation to major climate modes in historical and future Coupled Model Intercomparison Project Phase 5 simulations, Hydrol. Earth Syst. Sci., 24(3), 1131–1143, doi:10.5194/hess-24-1131-2020, 2020.

Le, T. and Bae, D.: Causal Links on Interannual Timescale Between ENSO and the IOD in CMIP5 Future Simulations, Geophys. Res. Lett., 46(5), 2820–2828, doi:10.1029/2018GL081633, 2019.

Le, T. and Bae, D.: Causal Impacts of El Niño–Southern Oscillation on Global Soil Moisture Over the Period 2015–2100, Earth's Futur., 10(3), doi:10.1029/2021EF002522, 2022a.

Le, T. and Bae, D.: Causal influences of El Niño–Southern Oscillation on global dust activities, Atmos. Chem. Phys., 22(8), 5253–5263, doi:10.5194/acp-22-5253-2022, 2022b.

Le, T., Ha, K.-J. J., Bae, D.-H. H. and Kim, S.-H. H.: Causal effects of Indian Ocean Dipole on El Niño-Southern Oscillation

during 1950-2014 based on high-resolution models and reanalysis data, Environ. Res. Lett., 15(10), 1040b6, doi:10.1088/1748-9326/abb96d, 2020a.

Le, T., Ha, K.-J., Bae, D.-H. and Kim, S.-H.: Causal effects of Indian Ocean Dipole on El Niño–Southern Oscillation during 1950–2014 based on high-resolution models and reanalysis data, Environ. Res. Lett., 15(10), 1040b6, doi:10.1088/1748-9326/abb96d, 2020b.

Le, T., Kim, S. and Bae, D.: Decreasing causal impacts of El Niño–Southern Oscillation on future fire activities, Sci. Total Environ., 826, 154031, doi:10.1016/j.scitotenv.2022.154031, 2022.

Li, X., Cai, W., Meehl, G. A., Chen, D., Yuan, X., Raphael, M., Holland, D. M., Ding, Q., Fogt, R. L., Markle, B. R., Wang, G., Bromwich, D. H., Turner, J., Xie, S. P., Steig, E. J., Gille, S. T., Xiao, C., Wu, B., Lazzara, M. A., Chen, X., Stammerjohn, S., Holland, P. R., Holland, M. M., Cheng, X., Price, S. F., Wang, Z., Bitz, C. M., Shi, J., Gerber, E. P., Liang, X., Goosse, H., Yoo, C., Ding, M., Geng, L., Xin, M., Li, C., Dou, T., Liu, C., Sun, W., Wang, X. and Song, C.: Tropical teleconnection impacts on Antarctic climate changes, Nat. Rev. Earth Environ., 2(10), 680–698, doi:10.1038/s43017-021-00204-5, 2021.

Lin, J. and Qian, T.: Impacts of the ENSO Lifecycle on Stratospheric Ozone and Temperature, Geophys. Res. Lett., 46(17–18), 10646–10658, doi:10.1029/2019GL083697, 2019.

Lin, M., Fiore, A. M., Horowitz, L. W., Langford, A. O., Oltmans, S. J., Tarasick, D. and Rieder, H. E.: Climate variability modulates western US ozone air quality in spring via deep stratospheric intrusions, Nat. Commun., 6(May), 1–11, doi:10.1038/ncomms8105, 2015.

Lin, M., Malyshev, S., Shevliakova, E., Paulot, F., Horowitz, L. W., Fares, S., Mikkelsen, T. N. and Zhang, L.: Sensitivity of Ozone Dry Deposition to Ecosystem-Atmosphere Interactions: A Critical Appraisal of Observations and Simulations, Global Biogeochem. Cycles, 33(10), 1264–1288, doi:10.1029/2018GB006157, 2019.

Liu, J., Rodriguez, J. M., Steenrod, S. D., Douglass, A. R., Logan, J. A., Olsen, M. A., Wargan, K. and Ziemke, J. R.: Causes of interannual variability over the southern hemispheric tropospheric ozone maximum, Atmos. Chem. Phys., 17(5), 3279–3299, doi:10.5194/acp-17-3279-2017, 2017.

Lu, X., Zhang, L. and Shen, L.: Meteorology and Climate Influences on Tropospheric Ozone: a Review of Natural Sources, Chemistry, and Transport Patterns, Curr. Pollut. Reports, 5(4), 238–260, doi:10.1007/s40726-019-00118-3, 2019.

Luo, J. J., Sasaki, W. and Masumoto, Y.: Indian Ocean warming modulates Pacific climate change, Proc. Natl. Acad. Sci. U. S. A., 109(46), 18701–18706, doi:10.1073/pnas.1210239109, 2012.

Lurton, T., Balkanski, Y., Bastrikov, V., Bekki, S., Bopp, L., Braconnot, P., Brockmann, P., Cadule, P., Contoux, C., Cozic, A., Cugnet, D., Dufresne, J. L., Éthé, C., Foujols, M. A., Ghattas, J., Hauglustaine, D., Hu, R. M., Kageyama, M., Khodri, M., Lebas, N., Levavasseur, G., Marchand, M., Ottlé, C., Peylin, P., Sima, A., Szopa, S., Thiéblemont, R., Vuichard, N. and Boucher, O.: Implementation of the CMIP6 Forcing Data in the IPSL-CM6A-LR Model, J. Adv. Model. Earth Syst., 12(4), 1–22, doi:10.1029/2019MS001940, 2020.

McPhaden, M. J., Zebiak, S. E. and Glantz, M. H.: ENSO as an integrating concept in earth science., Science, 314(December), 1740–1745, doi:10.1126/science.1132588, 2006.

Meul, S., Langematz, U., Kröger, P., Oberländer-Hayn, S. and Jöckel, P.: Future changes in the stratosphere-to-troposphere ozone mass flux and the contribution from climate change and ozone recovery, Atmos. Chem. Phys., 18(10), 7721–7738, doi:10.5194/acp-18-7721-2018, 2018.

Michou, M., Nabat, P., Saint-Martin, D., Bock, J., Decharme, B., Mallet, M., Roehrig, R., Séférian, R., Sénési, S. and Voldoire, A.: Present-Day and Historical Aerosol and Ozone Characteristics in CNRM CMIP6 Simulations, J. Adv. Model. Earth Syst., 12(1), 1–31, doi:10.1029/2019MS001816, 2020.

Mosedale, T. J., Stephenson, D. B., Collins, M. and Mills, T. C.: Granger Causality of Coupled Climate Processes: Ocean

Feedback on the North Atlantic Oscillation, J. Clim., 19(7), 1182–1194, doi:10.1175/JCLI3653.1, 2006.

Myhre, G., Shindell, D., Bréon, F.-M., Collins, W., Fuglestvedt, J., Huang, J., Koch, D., Lamarque, J.-F., Lee, D., Mendoza, B., Nakajima, T., Robock, A., Stephens, G., Takemura, T. and Zhan, H.: Anthropogenic and Natural Radiative Forcing: In Climate Change 2013: The Physical Science Basis. Contribution of Working Group I to the Fifth Assessment Report of the Intergovernmental Panel on Climate Change., 2013.

Neu, J. L., Flury, T., Manney, G. L., Santee, M. L., Livesey, N. J. and Worden, J.: Tropospheric ozone variations governed by changes in stratospheric circulation, Nat. Geosci., 7(5), 340–344, doi:10.1038/ngeo2138, 2014.

Oliver, R. J., Mercado, L. M., Sitch, S., Simpson, D., Medlyn, B. E., Lin, Y. S. and Folberth, G. A.: Large but decreasing effect of ozone on the European carbon sink, Biogeosciences, 15(13), 4245–4269, doi:10.5194/bg-15-4245-2018, 2018.

Olsen, M. A., Wargan, K. and Pawson, S.: Tropospheric column ozone response to ENSO in GEOS-5 assimilation of OMI and MLS ozone data, Atmos. Chem. Phys., 16(11), 7091–7103, doi:10.5194/acp-16-7091-2016, 2016.

Olsen, M. A., Manney, G. L. and Liu, J.: The ENSO and QBO Impact on Ozone Variability and Stratosphere-Troposphere Exchange Relative to the Subtropical Jets, J. Geophys. Res. Atmos., 124(13), 7379–7392, doi:10.1029/2019JD030435, 2019.

Oman, L. D., Ziemke, J. R., Douglass, A. R., Waugh, D. W., Lang, C., Rodriguez, J. M. and Nielsen, J. E.: The response of tropical tropospheric ozone to ENSO, Geophys. Res. Lett., 38(13), n/a-n/a, doi:10.1029/2011GL047865, 2011.

Oman, L. D., Douglass, A. R., Ziemke, J. R., Rodriguez, J. M., Waugh, D. W. and Nielsen, J. E.: The ozone response to ENSO in Aura satellite measurements and a chemistry-climate simulation, J. Geophys. Res. Atmos., 118(2), 965–976, doi:10.1029/2012JD018546, 2013.

Peiro, H., Emili, E., Cariolle, D., Barret, B. and Le Flochmoën, E.: Multi-year assimilation of IASI and MLS ozone retrievals: variability of tropospheric ozone over the tropics in response to ENSO, Atmos. Chem. Phys., 18(9), 6939–6958, doi:10.5194/acp-18-6939-2018, 2018.

Peron, A., Kaser, L., Charlott Fitzky, A., Graus, M., Halbwirth, H., Greiner, J., Wohlfahrt, G., Rewald, B., Sandén, H. and Karl, T.: Combined effects of ozone and drought stress on the emission of biogenic volatile organic compounds from Quercus robur L., Biogeosciences, 18(2), 535–556, doi:10.5194/bg-18-535-2021, 2021.

Raphael, M. N. and Holland, M. M.: Twentieth century simulation of the southern hemisphere climate in coupled models. Part 1: Large scale circulation variability, Clim. Dyn., 26(2–3), 217–228, doi:10.1007/s00382-005-0082-8, 2006.

Roberts, H. R., Dodd, I. C., Hayes, F. and Ashworth, K.: Chronic tropospheric ozone exposure reduces seed yield and quality in spring and winter oilseed rape, Agric. For. Meteorol., 316(August 2021), 108859, doi:10.1016/j.agrformet.2022.108859, 2022.

Rowlinson, M. J., Rap, A., Arnold, S. R., Pope, R. J., Chipperfield, M. P., McNorton, J., Forster, P., Gordon, H., Pringle, K. J., Feng, W., Kerridge, B. J., Latter, B. L. and Siddans, R.: Impact of El Niño–Southern Oscillation on the interannual variability of methane and tropospheric ozone, Atmos. Chem. Phys., 19(13), 8669–8686, doi:10.5194/acp-19-8669-2019, 2019.

Saji, N. H., Goswami, B. N., Vinayachandran, P. N. and Yamagata, T.: A dipole mode in the tropical Indian Ocean, Nature, 401(6751), 360–363, doi:10.1038/43854, 1999.

Schauberger, B., Rolinski, S., Schaphoff, S. and Müller, C.: Global historical soybean and wheat yield loss estimates from ozone pollution considering water and temperature as modifying effects, Agric. For. Meteorol., 265(October 2018), 1–15, doi:10.1016/j.agrformet.2018.11.004, 2019.

Schwarz, G.: Estimating the dimension of a model, Ann. Stat. [online] Available from: http://projecteuclid.org/euclid.aos/1176344136 (Accessed 30 May 2014), 1978.

Sekiya, T. and Sudo, K.: Role of meteorological variability in global tropospheric ozone during 1970-2008, J. Geophys. Res.

Atmos., 117(17), 1–16, doi:10.1029/2012JD018054, 2012.

Stern, D. I. and Kaufmann, R. K.: Anthropogenic and natural causes of climate change, Clim. Change, 122(1–2), 257–269, doi:10.1007/s10584-013-1007-x, 2013.

Stocker, T. F., Qin, D., Plattner, G.-K., Alexander, L. V., Allen, S. K., Bindoff, N. L., Bréon, F.-M., Church, J. A., Cubasch, U., Emori, S., Forster, P., Friedlingstein, P., Gillett, N., Gregory, J. M., Hartmann, D. L., Jansen, E., Kirtman, B., Knutti, R., Kumar, K. K., Lemke, P., Marotzke, J., Masson-Delmotte, V. Meehl, G. A., Mokhov, I. I., Piao, S., Ramaswamy, V., Randall, D., Rhein, M., Rojas, M., Sabine, C., Shindell, D., Talley, L. D., Vaughan, D. G. and Xie, S.-P.: Technical Summary, in Climate Change 2013 - The Physical Science Basis, edited by Intergovernmental Panel on Climate Change, pp. 31–116, Cambridge University Press, Cambridge., 2013.

Turnock, S. T., Allen, R. J., Andrews, M., Bauer, S. E., Deushi, M., Emmons, L., Good, P., Horowitz, L., John, J. G., Michou, M., Nabat, P., Naik, V., Neubauer, D., O'Connor, F. M., Olivié, D., Oshima, N., Schulz, M., Sellar, A., Shim, S., Takemura, T., Tilmes, S., Tsigaridis, K., Wu, T. and Zhang, J.: Historical and future changes in air pollutants from CMIP6 models, Atmos. Chem. Phys., 20(23), 14547–14579, doi:10.5194/acp-20-14547-2020, 2020.

Verstraeten, W. W., Neu, J. L., Williams, J. E., Bowman, K. W., Worden, J. R. and Boersma, K. F.: Rapid increases in tropospheric ozone production and export from China, Nat. Geosci., 8(9), 690–695, doi:10.1038/ngeo2493, 2015.

Wang, T., Xue, L., Feng, Z., Dai, J., Zhang, Y. and Tan, Y.: Ground-level ozone pollution in China: a synthesis of recent findings on influencing factors and impacts, Environ. Res. Lett., 17(6), 063003, doi:10.1088/1748-9326/ac69fe, 2022.

Wespes, C., Hurtmans, D., Clerbaux, C. and Coheur, P. -F.: O 3 variability in the troposphere as observed by IASI over 2008–2016: Contribution of atmospheric chemistry and dynamics, J. Geophys. Res. Atmos., 122(4), 2429–2451, doi:10.1002/2016JD025875, 2017.

Wie, J., Moon, B.-K., Yeh, S.-W., Park, R. J. and Kim, B.-G.: La Niña-related tropospheric column ozone enhancement over East Asia, Atmos. Environ., 261(October 2020), 118575, doi:10.1016/j.atmosenv.2021.118575, 2021.

Williams, R. S., Hegglin, M. I., Kerridge, B. J., Jöckel, P., Latter, B. G. and Plummer, D. A.: Characterising the seasonal and geographical variability in tropospheric ozone, stratospheric influence and recent changes, Atmos. Chem. Phys., 19(6), 3589–3620, doi:10.5194/acp-19-3589-2019, 2019.

Wu, T., Lu, Y., Fang, Y., Xin, X., Li, L., Li, W., Jie, W., Zhang, J., Liu, Y., Zhang, L., Zhang, F., Zhang, Y., Wu, F., Li, J., Chu, M., Wang, Z., Shi, X., Liu, X., Wei, M., Huang, A., Zhang, Y. and Liu, X.: The Beijing Climate Center Climate System Model (BCC-CSM): The main progress from CMIP5 to CMIP6, Geosci. Model Dev., 12(4), 1573–1600, doi:10.5194/gmd-12-1573-2019, 2019.

Xu, L., Yu, J.-Y., Schnell, J. L. and Prather, M. J.: The seasonality and geographic dependence of ENSO impacts on U.S. surface ozone variability, Geophys. Res. Lett., 44(7), 3420–3428, doi:10.1002/2017GL073044, 2017.

Yang, Y., Li, M., Wang, H., Li, H., Wang, P., Li, K., Gao, M. and Liao, H.: ENSO modulation of summertime tropospheric ozone over China, Environ. Res. Lett., 17(3), 034020, doi:10.1088/1748-9326/ac54cd, 2022.

Yeh, S.-W., Cai, W., Min, S.-K., McPhaden, M. J., Dommenget, D., Dewitte, B., Collins, M., Ashok, K., An, S.-I., Yim, B.-Y. and Kug, J.-S.: ENSO Atmospheric Teleconnections and Their Response to Greenhouse Gas Forcing, Rev. Geophys., 56(1), 185–206, doi:10.1002/2017RG000568, 2018.

Young, P. J., Naik, V., Fiore, A. M., Gaudel, A., Guo, J., Lin, M. Y., Neu, J. L., Parrish, D. D., Rieder, H. E., Schnell, J. L., Tilmes, S., Wild, O., Zhang, L., Ziemke, J., Brandt, J., Delcloo, A., Doherty, R. M., Geels, C., Hegglin, M. I., Hu, L., Im, U., Kumar, R., Luhar, A., Murray, L., Plummer, D., Rodriguez, J., Saiz-Lopez, A., Schultz, M. G., Woodhouse, M. T. and Zeng, G.: Tropospheric Ozone Assessment Report: Assessment of global-scale model performance for global and regional ozone distributions, variability, and trends, edited by D. Helmig and A. Lewis, Elem. Sci. Anthr., 6, doi:10.1525/elementa.265, 2018.

Zanis, P., Akritidis, D., Turnock, S., Naik, V., Szopa, S., Georgoulias, A. K., Bauer, S. E., Deushi, M., Horowitz, L. W., Keeble, J., Le Sager, P., O'Connor, F. M., Oshima, N., Tsigaridis, K. and van Noije, T.: Climate change penalty and benefit on surface ozone: a global perspective based on CMIP6 earth system models, Environ. Res. Lett., 17(2), 024014, doi:10.1088/1748-9326/ac4a34, 2022.

Zeng, G. and Pyle, J. A.: Influence of El Niño Southern Oscillation on stratosphere/troposphere exchange and the global tropospheric ozone budget, Geophys. Res. Lett., 32(1), L01814, doi:10.1029/2004GL021353, 2005.

Zhang, J., Tian, W., Xie, F., Li, Y., Wang, F., Huang, J. and Tian, H.: Influence of the El Niño southern oscillation on the total ozone column and clear-sky ultraviolet radiation over China, Atmos. Environ., 120, 205–216, doi:10.1016/j.atmosenv.2015.08.080, 2015.

Ziemke, J. R. and Chandra, S.: La Nina and El Nino - Induced variabilities of ozone in the tropical lower atmosphere during 1970-2001, Geophys. Res. Lett., 30(3), 30–33, doi:10.1029/2002GL016387, 2003.

Ziemke, J. R., Douglass, A. R., Oman, L. D., Strahan, S. E. and Duncan, B. N.: Tropospheric ozone variability in the tropics from ENSO to MJO and shorter timescales, Atmos. Chem. Phys., 15(14), 8037–8049, doi:10.5194/acp-15-8037-2015, 2015.

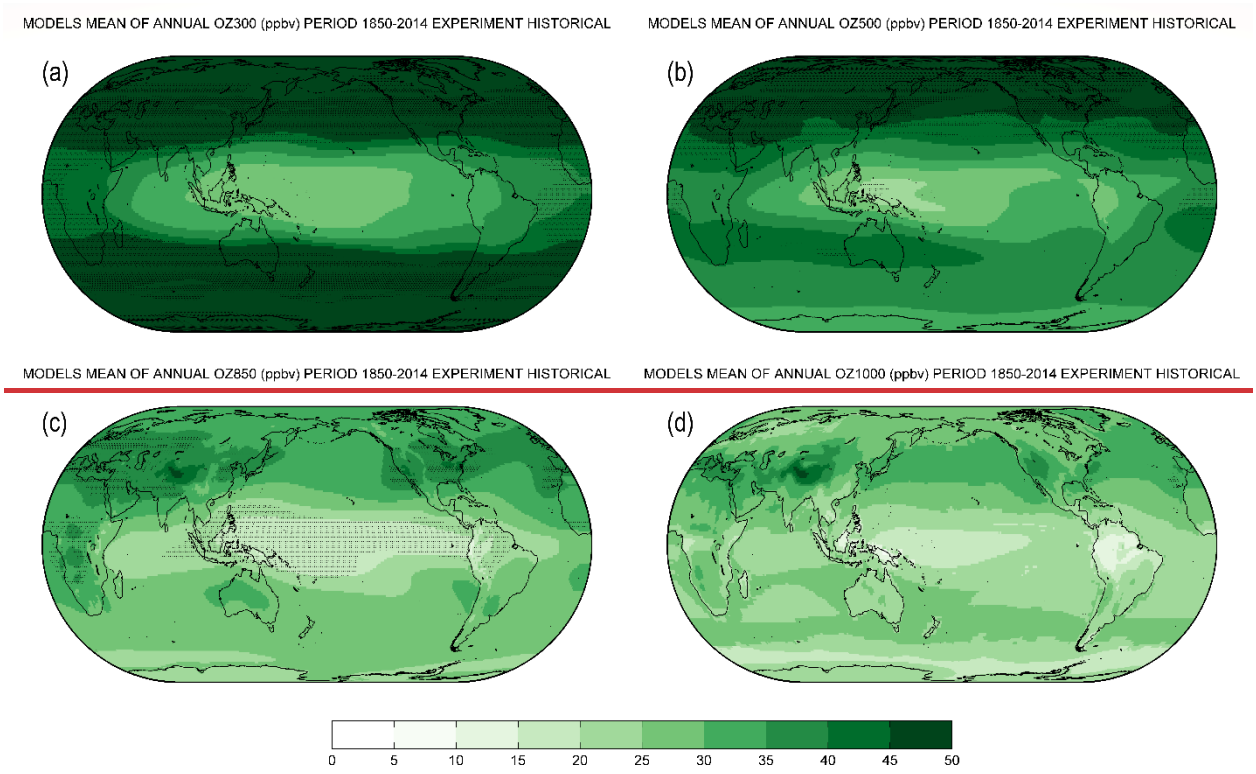
MODELS MEAN OF ANNUAL OZ300 (ppbv) PERIOD 1850-2014 EXPERIMENT HISTORICAL
MODELS MEAN OF ANNUAL OZ500 (ppbv) PERIOD 1850-2014 EXPERIMENT HISTORICAL
(a)
(b)
MODELS MEAN OF ANNUAL OZ850 (ppbv) PERIOD 1850-2014 EXPERIMENT HISTORICAL
MODELS MEAN OF ANNUAL OZ1000 (ppbv) PERIOD 1850-2014 EXPERIMENT HISTORICAL
(c)
(d)
0
5
10
15
20
25
30
35
40
45
50

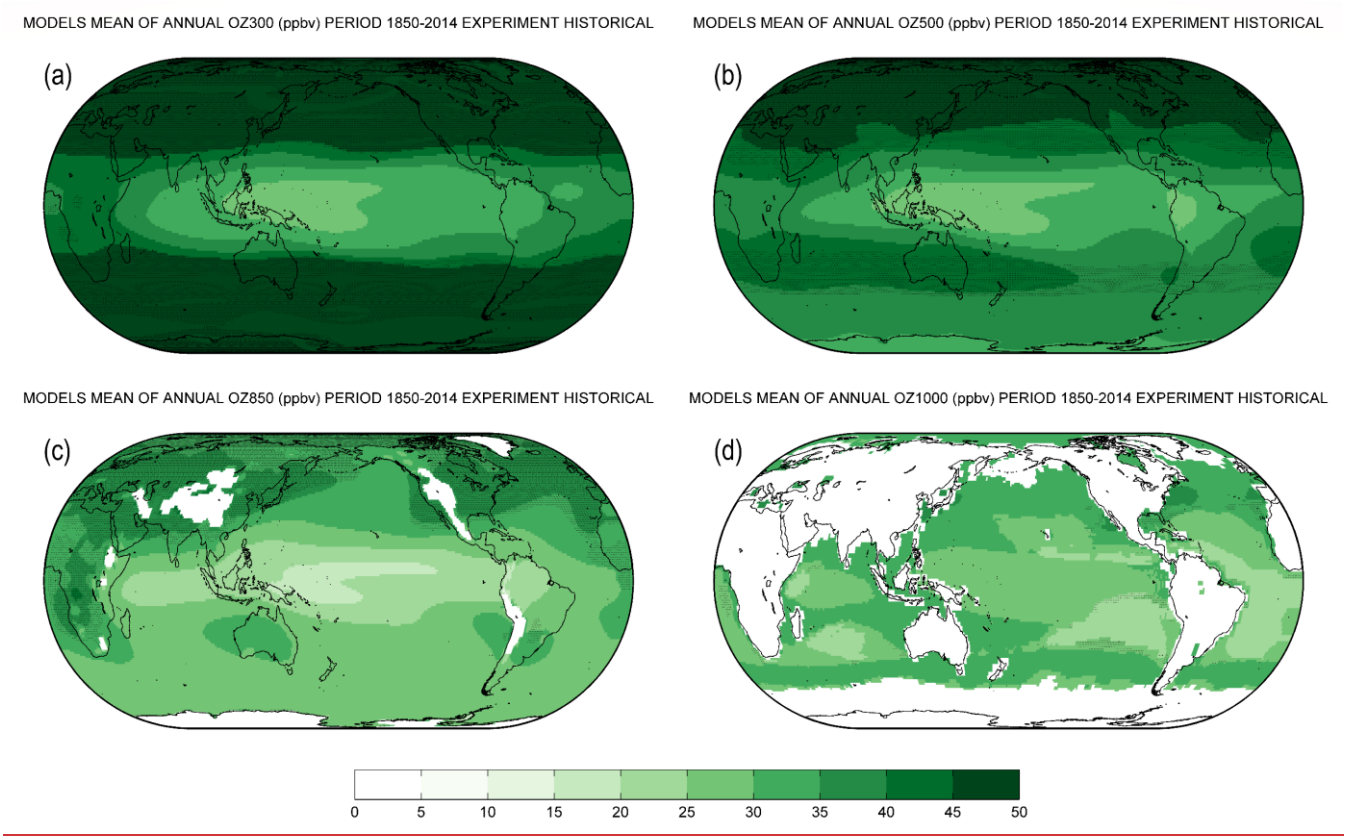

Figure 1. Multi-model mean map of annual mean ozone concentrations (ppbv) for the historical experiment over the 1850-2014 period at 300 hPa (a), 500 hPa (b), 850 hPa (c) and 1000 hPa (d) pressure levels, respectively. Stippling indicates that at least 70% of total models show agreement on the mean ozone concentrations of all models at given grid point. The agreement of an individual model is identified when the difference between the selected model's ozone concentrations and the multi-model mean ozone concentrations is less than one standard deviation of the multi-model mean ozone concentrations.

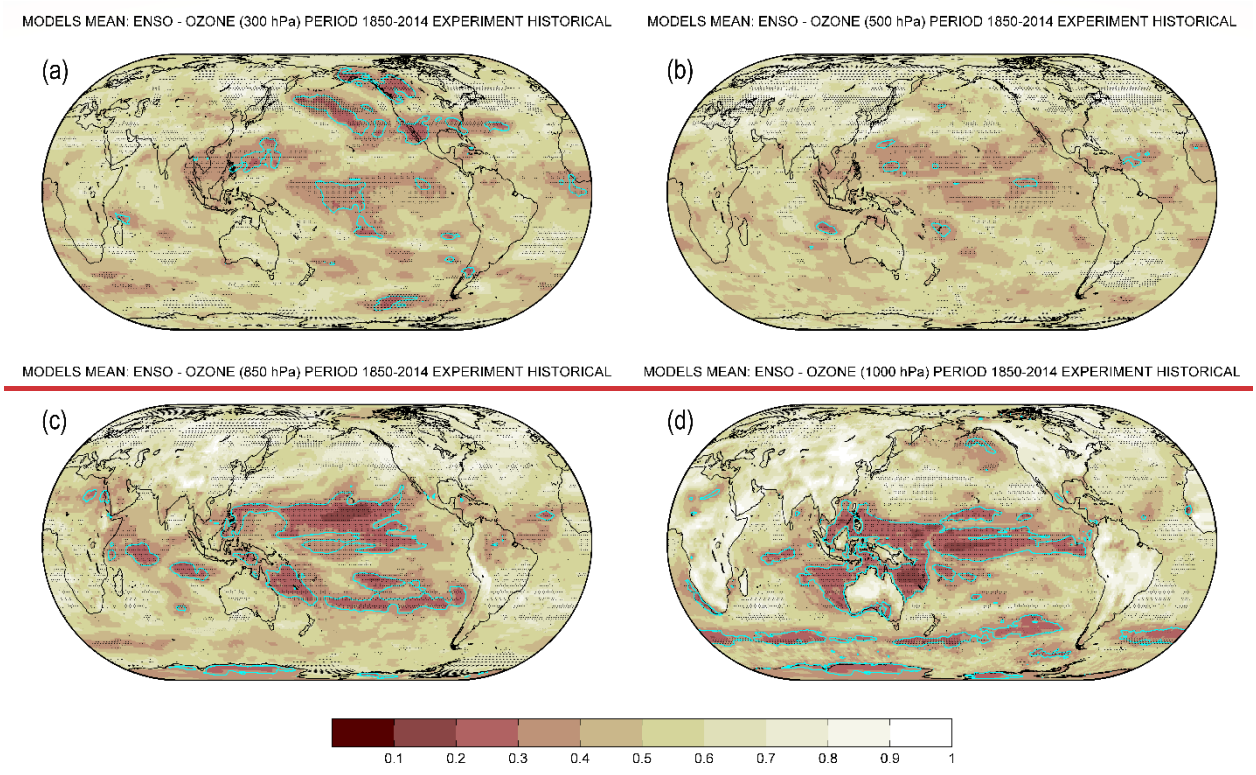
MODELS MEAN: ENSO - OZONE (300 hPa) PERIOD 1850-2014 EXPERIMENT HISTORICAL
MODELS MEAN: ENSO - OZONE (500 hPa) PERIOD 1850-2014 EXPERIMENT HISTORICAL
(a)
(b)
MODELS MEAN: ENSO - OZONE (850 hPa) PERIOD 1850-2014 EXPERIMENT HISTORICAL
MODELS MEAN: ENSO - OZONE (1000 hPa) PERIOD 1850-2014 EXPERIMENT HISTORICAL
(c)
(d)
0.1
0.2
0.3
0.4
0.5
0.6
0.7
0.8
0.9
1

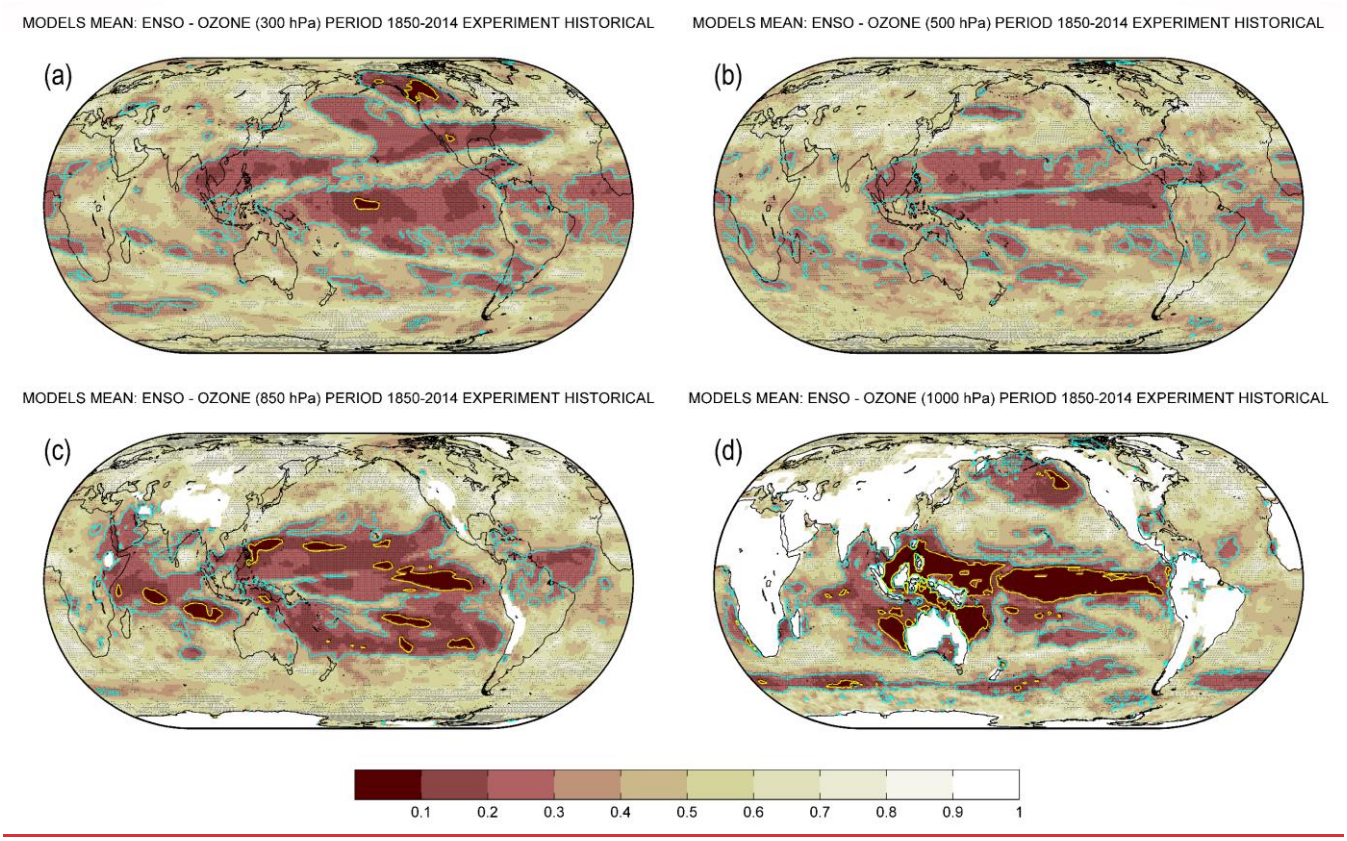

Figure 2. Map of multi-model mean probability for the absence of Granger causality from ENSO to annual ozone concentrations for the historical experiment over the 1850-2014 period at 300 hPa (a), 500 hPa (b), 850 hPa (c) and 1000 hPa (d) pressure levels, respectively. Stippling indicates that at least 70% of total models show agreement on the mean probability of all models at given grid point. The agreement of an individual model is identified when the difference between the selected model's probability and the multi-model mean probability is less than one standard deviation of the multi-model mean probability. The cyan and yellow contour lines denote~~s~~ *p*-value = 0.33 and 0.1, respectively. Brown shades indicate low probability of no Granger causality. ENSO = El Niño–Southern Oscillation.

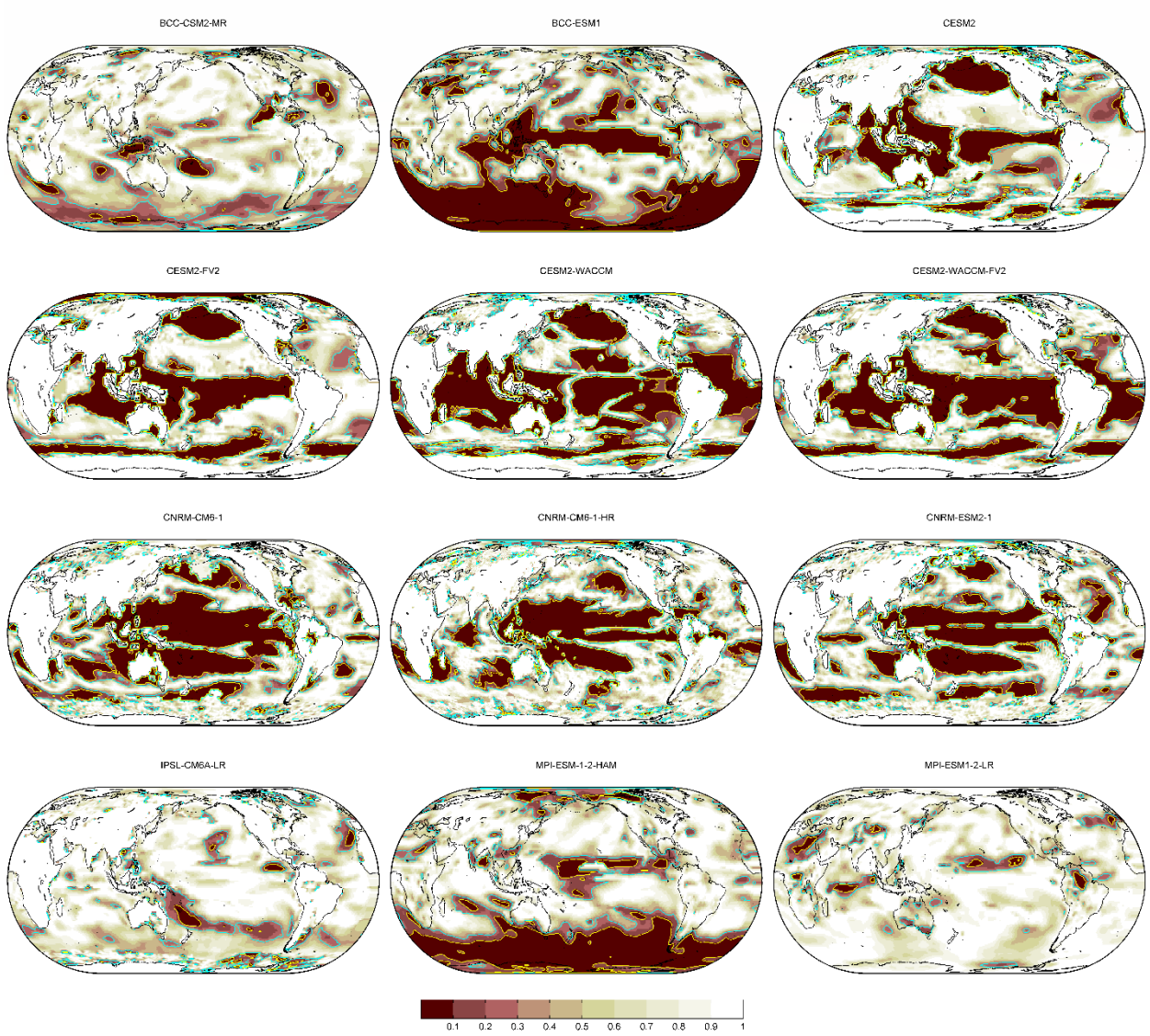

Figure 3. Probability of no Granger causality from ENSO to annual ozone concentrations at 1000 hPa pressure level for the historical experiment over the 1850-2014 period of 12 individual models (see Table 1). The yellow and cyan contour lines denote *p*-value = 0.1 and 0.33, respectively. Brown shades imply a low probability of no Granger causality. ENSO: El Niño–Southern Oscillation.

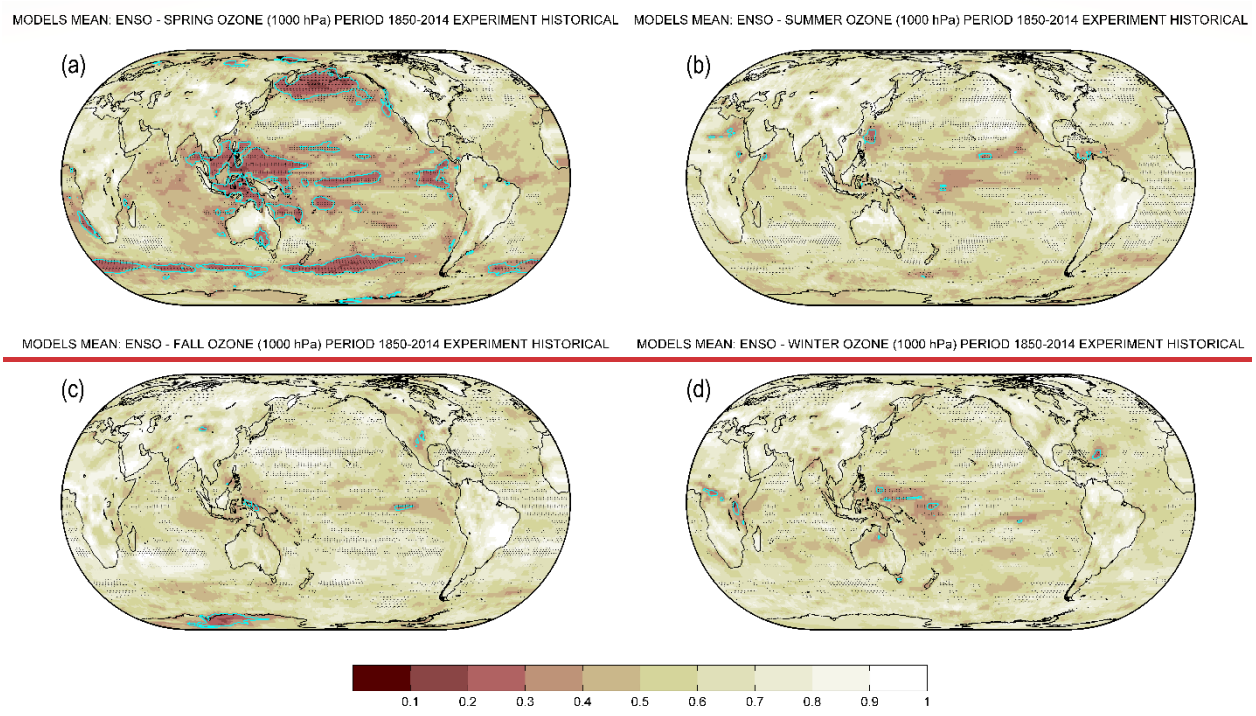
MODELS MEAN: ENSO - SPRING OZONE (1000 hPa) PERIOD 1850-2014 EXPERIMENT HISTORICAL
MODELS MEAN: ENSO - SUMMER OZONE (1000 hPa) PERIOD 1850-2014 EXPERIMENT HISTORICAL
(a)
(b)
MODELS MEAN: ENSO - FALL OZONE (1000 hPa) PERIOD 1850-2014 EXPERIMENT HISTORICAL
MODELS MEAN: ENSO - WINTER OZONE (1000 hPa) PERIOD 1850-2014 EXPERIMENT HISTORICAL
(c)
(d)
0.1 0.2 0.3 0.4 0.5 0.6 0.7 0.8 0.9 1

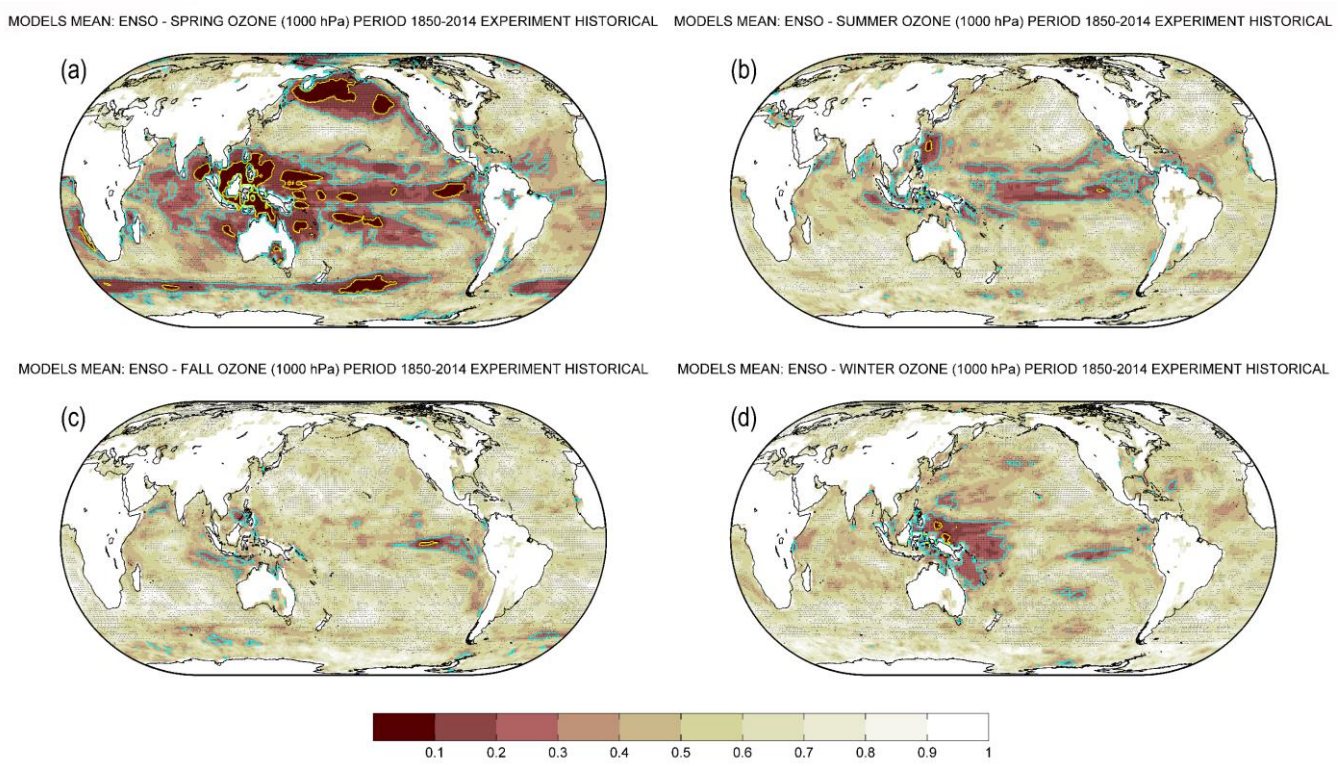
MODELS MEAN: ENSO - SPRING OZONE (1000 hPa) PERIOD 1850-2014 EXPERIMENT HISTORICAL
MODELS MEAN: ENSO - SUMMER OZONE (1000 hPa) PERIOD 1850-2014 EXPERIMENT HISTORICAL
(a)
(b)
MODELS MEAN: ENSO - FALL OZONE (1000 hPa) PERIOD 1850-2014 EXPERIMENT HISTORICAL
MODELS MEAN: ENSO - WINTER OZONE (1000 hPa) PERIOD 1850-2014 EXPERIMENT HISTORICAL
(c)
(d)
0.1 0.2 0.3 0.4 0.5 0.6 0.7 0.8 0.9 1

Figure 4. Multi-model mean probability map of no Granger causality from ENSO in boreal winter [D(*t*)JF(*t+1*); *t* indicates year *t*] to seasonal mean ozone concentrations at 1000 hPa pressure level over the period 1850-2014. (a) Spring [MAM(*t+1*)]. (b) Summer [JJA(*t+1*)]. (c) Fall [SON(*t+1*)]. (d) Winter [D(*t+1*)JF(*t+2*)]. Stippling signifies that at least 70% of total models show agreement on the mean probability of all models at a given grid point. The cyan contour line signifies *p*-value = 0.33. Brown shades imply a low probability of no Granger causality. ENSO: El Niño–Southern Oscillation. MAM: March- April-May. JJA: June-July-August. SON: September-October-November. DJF: December-January-February.